The DFT Route to NMR Chemical Shifts

MICHAEL BÜHL,[1] MARTIN KAUPP,[2] OLGA L. MALKINA[3,4] VLADIMIR G. MALKIN,[3]

[1] *Universität Zürich, Organisch-chemisches Institut, Winterthurerstr. 190, CH-8057 Zürich, Switzerland*
[2] *Max-Planck-Institut für Festkörperforschung, Heisenbergstr. 1, D-70569 Stuttgart, Germany*
[3] *Institute of Inorganic Chemistry, Slovak Academy of Sciences, Dubravska Cesta 9, SK-84236 Bratislava, Slovakia*
[4] *Computing Center, Slovak Academy of Sciences, Dubravska Cesta 9, SK-84236 Bratislava, Slovakia*

Received 14 June 1998; accepted accepted 15 July 1998

ABSTRACT: An overview is given of the recent development and use of density functional methods in nuclear magnetic resonance (NMR) chemical-shift calculations. The available density functional theory (DFT) methods are discussed, and examples for their validation and application are given. Relativistic effects are also considered, with an emphasis on spin–orbit coupling. The systems discussed range from transition-metal complexes and clusters via biological systems and fullerenes to weakly bound van der Waals molecules. DFT results not published previously comprise spin–orbit effects on ^{31}P chemical shifts in phosphorus halides, the orientation of the ^{31}P-shift tensor in $Ru_4(PPh)(CO)_{13}$, $\delta(^{95}Mo)$ data, ^{13}C and endohedral chemical shifts for fullerenes and for $C_{60}H_{36}$, as well as the shielding surface of the Ne_2 molecule. © 1999 John Wiley & Sons, Inc. J Comput Chem 20: 91–105, 1999

Keywords: density functional theory; fullerenes; NMR chemical shifts; relativistic effects; transition metal compounds; van-der-Waals complexes

Introduction

A wealth of information is encoded in the multinuclear NMR spectra of a given compound. Consequently, it is of great interest to compute and analyze the observable quantities of an NMR spectrum from first principles. Most applications of quantum-chemical methods to NMR spectroscopy, in particular those involving the lighter nuclei of the first two periods, concentrate on the extraction of structural parameters from the NMR data. In addition, the NMR properties reflect the particular electronic structure of a molecule and may help to rationalize other properties such as reactivities.

The area of theoretical and computational chemistry dealing with NMR properties is blossoming

Correspondence to: Any of the authors

Contract/grant sponsor: Fonds der Chemischen Industrie, contract/grant sponsor: Deutsche Forschungsgemeinschaft; contract/grant sponsor: Slovak Grant Agency VEGA, contract/grant number: 2/3008/98

© 1999 John Wiley & Sons, Inc.
CCC 0192-8651 / 99 / 010091-15

and today's chemists have a diversified arsenal of methods at their disposal, which allows the calculation of these parameters from first principles. The most progress has been achieved during the past decade in the calculation of NMR chemical shifts. The establishment of variants of the coupled Hartree–Fock (CHF) method with distributed gauge origins (e.g., the IGLO and GIAO approaches) has been a breakthrough in the field of NMR chemical-shift calculations, as systems of chemically significant size became accessible to quantitative treatment. The continuing progress in this field has been reviewed.[1,2] During the past 5 years, powerful post-Hartree–Fock approaches for the inclusion of electron correlation in chemical shift calculations have been developed.[3] Unfortunately, the computational expense of these correlated methods precludes their routine application to many problems of chemical interest.

Density-functional theory (DFT) is now established as a viable alternative to conventional *ab initio* methods. This also holds for the description of magnetic properties: It has been found during the past few years that relatively simple and computationally inexpensive DFT approaches for the calculation of NMR chemical shifts often give surprisingly accurate and stable results, even in cases such as transition-metal compounds,[4] which are known to exhibit strong correlation effects.[5] This has opened the way for a steadily increasing number of applications, which are the topic of this article. Our intention is to present a brief overview of what can be done with state-of-the-art DFT methods for the computation of NMR chemical shifts and what can be learned from the results. Current limitations will be noted in passing because it is also important to be aware of what cannot yet be done.

We restrict the discussion to diamagnetic closed-shell systems, as truly quantitative calculations of chemical shifts for paramagnetic compounds have not yet been reported. We will first briefly outline the available DFT approaches, calling special attention to relativistic effects. Applications of these methods will be highlighted for transition-metal compounds, for large systems, and for van der Waals molecules. The choice of examples is, as always, a subjective one without the claim of completeness, and may serve to complement those discussed in recent overviews on similar subjects.[4,6] We also provide some examples that have not previously been published. A summary and a perspective for future work are given in the final section.

DFT Methods for the Calculation of NMR Chemical Shifts

The major appeal of DFT in many areas of chemistry and physics is the implicit inclusion of electron correlation via the exchange-correlation functional, at comparable computational cost to a HF treatment.[7] However, the basic DFT theorem of Hohenberg and Kohn was formulated for a system in the absence of a magnetic field. Taking the latter into account leads to further complications, because the exchange-correlation functional should depend on the magnetic field.[8] Thus, one would need current-dependent (or magnetic-field-dependent) exchange-correlation functionals. A recent implementation of such a current-density functional theory[9] (CDFT) has been carried out by Handy and coworkers.[10] Within the model used, they found that the current-dependent contributions to chemical shifts were very small and did not improve the results.[11] Two other models have been suggested, by Becke[12] and by Capelle and Gross,[13] but we are not aware of any implementation or results of these new models. More work is needed in this area.

Is it possible (or sensible) to neglect the current-dependent terms altogether, by employing the usual local or gradient-corrected exchange-correlation functionals in conjunction with stationary perturbation theory? This approach has become popular and is implemented in many codes. At the HF level, stationary perturbation theory leads to the well-known coupled Hartree–Fock (CHF) equations (see, e.g., ref. 2); in contrast, the Kohn–Sham procedure gives uncoupled DFT equations (UDFT). In this case, the magnetic Hessian is diagonal in the Kohn–Sham orbitals, due to the fact that these energy functionals do not depend on the current density induced by the magnetic field. A discussion of the relation between several of the approaches mentioned has been given[14] (also note ref. 15 for a different approach).

In many cases, this UDFT method without current-dependent terms already gives surprisingly good chemical shifts. It seems that the Kohn–Sham orbitals form a considerably better basis for perturbation treatment than, for instance, the HF orbitals,[16] and that coupling terms are thus small.[17] This was not clear from early implementations of DFT methods for the calculation of chemical shifts, which were plagued by small basis sets and the restriction to the X_α potential.[18] The first efficient

implementation of such a UDFT approach used the IGLO choice of gauge origin.[19] Good accuracy has been found for the chemical shifts in light-atom systems; for example, in organic compounds. Meanwhile, several gauge-including-atomic-orbital (GIAO)[10,20–22] and localized-orbital-local-gauge-origin (LORG)[23] implementations of the UDFT approach exist as well.

In spite of the overall good agreement with experiment, the UDFT computations often tend to overestimate the paramagnetic terms somewhat, in particular when the latter are dominated by large individual excitation contributions, typically for systems with low-lying excited states. It is presently unclear to what extent this is due to general deficiencies of the existing density functionals or to the neglect of current-dependent terms. To overcome such problems, Malkin et al.[24,25] took advantage of a sum-over-states representation of the UDFT equations to introduce a correction term into the energy denominator of the expression for the paramagnetic part of the shielding tensor. A number of different expressions for this correction have been obtained from considerations of the residual exchange interactions between a hole created in ψ_k and the electron transferred to ψ_a.[24,25] This modified approach has been termed sum-over-states density-functional perturbation theory (SOS-DFPT); in many cases, it improves the agreement with experiment, because the paramagnetic terms are reduced.[24,25] If the correction term is omitted, the UDFT approach is obtained.

Studies of main-group species using both the UDFT and the SOS-DFPT approaches reveal that different gradient-corrected density functionals give similar agreement with experimental chemical shifts, whereas local density functionals perform, by and large, significantly worse.[19,24,25] A new consideration arises when so-called hybrid functionals are used, in which some fraction of local exchange is replaced by exact HF exchange (as, e.g., in the popular B3LYP functional). According to the implementation for hybrid functionals within the Gaussian-94 program, the CHF-type equations are solved considering couplings only from the HF nonlocal exchange operator.[22] No coupling terms are included from the pure DFT exchange-correlation part (the two different contributions are weighted according to the relative proportion of ''exact'' and local exchange in the hybrid functional used).

Basis set requirements for DFT-GIAO and DFT-IGLO computations of NMR chemical shifts are similar to those for the corresponding CHF-type calculations; that is, less than for post-CHF approaches. Different implementations of DFT methods further differ with respect to the treatment of the Coulomb and exchange-correlation contributions. Some programs make use of auxiliary basis sets for an expansion of only the Coulomb term or, alternatively, of both terms, to reduce the formal scaling of the method from N^4 to N^3 (N is the number of basis functions). These approaches are less expensive computationally, but the auxiliary basis sets used are further potential error sources that have to be controlled carefully. Moreover, the grids used for the numerical integrations in DFT calculations also require some attention.

Importance of Relativistic Effects for Chemical Shifts

Due to the computational expediency, and in view of the implicit inclusion of electron correlation, the application of DFT approaches appears particularly attractive for heavy-element compounds. This requires, however, that relativistic effects are dealt with adequately, as these are expected to be of particular importance in the presence of heavier atoms. We may discriminate between spin-free (''scalar'') relativistic effects and spin–orbit coupling.[26] The methods available at the moment to include such relativistic contributions into NMR property computations have already been discussed in more detail in two recent reviews.[4,6] Thus, we only mention here that scalar relativistic effects on light nuclei in the vicinity of heavier atoms may be treated very conveniently by replacing the core electrons of the heavy atoms with quasirelativistic effective-core potentials (ECPs).[4,5,27,28] Alternatively, Schreckenbach and Ziegler have implemented a first-order perturbational approach to include the scalar relativistic effects, combined with the frozen-core approximation.[29] Other relativistic calculations of chemical shifts at the finite-perturbation theory (FPT) HF level by Nakatsuji and coworkers[30] have employed a no-pair Hamiltonian. A very recent, preliminary study at the Dirac–Fock level has also appeared.[31] Undoubtedly, these and other relativistic all-electron Hamiltonians (also, e.g., the zero-order regular approximation[32]) will also be used in the future for relativistic chemical shielding calculations within a DFT framework. This is particularly important in view of the need to ac-

count for relativistic effects and for electron correlation at the same time. The scalar relativistic effects become particularly important when one descends to the sixth period, and thus their inclusion into the calculations is mandatory. This has meanwhile been demonstrated in a variety of cases,[5, 27, 29, 30] and has also been reviewed.[4, 6]

Considerable progress has been made very recently in the understanding of spin–orbit (SO) effects on chemical shifts,[33] and DFT methods have been very important as a computational basis. There are different ways of including SO contributions into chemical-shift calculations. Within a Kohn–Sham framework, it has been shown that a relatively inexpensive third-order perturbation treatment of SO corrections to nuclear shieldings (based on nonrelativistic Kohn–Sham orbitals) is possible by including the FC part of the hyperfine interactions (which is important, due to the SO-induced spin polarization) by FPT.[34] Based on the spin-polarized MOs, a modified UDFT or SOS-DFPT approach is then employed.

This particular approach is closely related to a previously described FPT-DFT ansatz[35] for the calculation of the FC contribution to indirect spin–spin coupling. Indeed, the comparison of these two perturbation theoretical approaches leads to the realization that the SO contributions to chemical shifts (''spin–orbit shifts''[33]) exhibit a close analogy to the FC contribution to indirect spin–spin coupling.[33] Consider the qualitative interaction scenario in Figure 1. In Figure 1a, the SO shifts are indicated to be caused by the spin-orbit operator on the heavy atom A, which in the presence of an external magnetic field B_0 leads to a small amount of electronic spin polarization. The latter may now interact with the nuclear magnetic moments (e.g., nucleus B) in the system, mainly via an FC mechanism, and will cause a change in their nuclear shieldings. Similarly, Figure 1b shows that FC interactions lead to spin–spin coupling between nuclei A and B via an intermediate electronic spin polarization. The left sides of the two schemes are essentially identical, whereas the right sides differ. Thus, we may expect that changes on the left side may affect the two quantities (i.e. SO shifts and spin–spin coupling) in an analogous way. This analogy, which had already been implied many years ago by Nakagawa et al.,[36] has recently been confirmed[33] by explicit SOS-DFPT calculations on some compounds bearing one iodine substituent. For instance, it was found that long-range SO shifts in iodobenzene show the same oscillations, with increasing numbers of intervening bonds, as

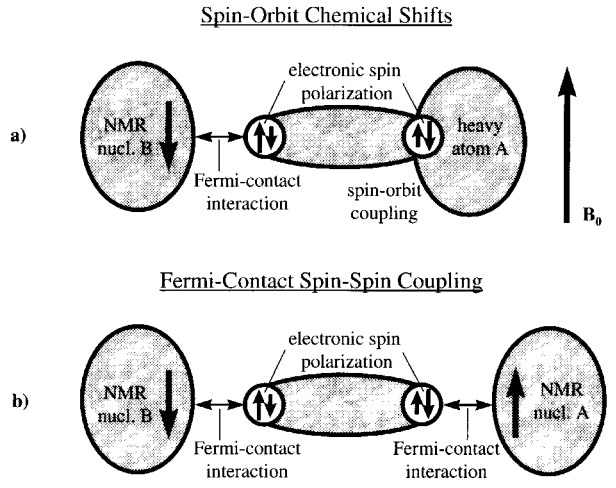

FIGURE 1. Schematic illustration of the suggested analogy between spin–orbit shifts and the Fermi-contact mechanism of indirect spin–spin coupling (cf. ref. 33 for details). (a) Qualitative interaction mechanism for spin–orbit shifts. (b) Qualitative Fermi-contact interaction mechanism for spin–spin coupling.

the spin–spin coupling constants. Similarly, a Karplus-type relation was found for SO shifts across three bonds as a function of the dihedral angle.[33]

Perhaps most importantly, the SO-shift/spin–spin coupling analogy implies that SO shifts will depend strongly on the s-character of the bonding around the atom observed by NMR spectroscopy, as the FC mechanism acts via the spherical part of the density at the nucleus. This dependency on s-character has indeed been demonstrated, and is particularly apparent for SO shifts across one bond; for instance, for the sp^3-, sp^2-, and sp-hybridized α-carbon atoms in iodoethane, iodoethylene (iodobenzene), and iodoacetylene, respectively.[33] The importance of the s-character has far-reaching consequences for SO-induced heavy-atom effects on chemical shifts. Among other things, it explains why chemical shifts of main-group elements in their highest oxidation states exhibit very large SO shifts when attached to halogen or related substituents. The s-character of the bonding to the heavy-atom substituents is large in such cases, and thus there exists an efficient FC mechanism that transfers the SO-induced spin polarization to the ''NMR nucleus.''

Because the SO shifts due to halogen substituents are usually shielding, and their magnitude increases with the atomic number of the halogen, the consequence is a large increase of the nuclear shielding of the central atom when going from

Cl to Br to I substituents. This is usually called a ''normal halogen dependence'' (NHD),[37] but the same behavior also holds (e.g., chalcogen substituents). Figure 2 shows an example of such behavior for the ^{31}P shieldings in the phosphorus(V)oxytrihalides POX_3 (X = F, Cl, Br). A U-shaped curve is typical for such plots, due to the onset of significant SO effects after X = Cl.[34,37,38] However, a very different behavior is exhibited by the ^{31}P shieldings of the phosphorus(III)trihalides, PX_3, also plotted in Figure 2. Here the SO shifts are much smaller, in spite of the fact that the phosphorus centers in both the PX_3 and POX_3 species bear three halogen substituents. The reason is that the phosphorus 3s-character in PX_3 is largely concentrated in the nonbonding electron pair, whereas the P—X bonds are dominated essentially by the phosphorus 3p orbitals. As a result, the computed SO-corrected ^{31}P shieldings of PCl_3 and PBr_3 are quite similar, as found experimentally. Likewise, other main group compounds in low oxidation states even exhibit appreciable ''inverse halogen dependence'' (IHD), which is probably in part due to the lack of significant SO effects. ^{119}Sn and ^{207}Pb shifts of tin(II) and lead(II) halides in the solid state[39] may serve as examples, as well as ^{27}Al shifts of Al(I) halides in solution.[40] Ligand SO effects on transition-metal shieldings are also expected (and found[41,42]) to be relatively small, in view of the relatively small s-character of the bonds. Indeed, IHD is generally found for early transition-metal halides.[37,43] Although NHD is again found for later transition metals, our preliminary findings indicate that this is only to a minor part caused by SO effects (of course, for d^{10} complexes the s-character is again large, and SO effects are expected to be significant). Finally, we note that: (a) SO contributions to chemical shifts may also be deshielding (e.g., for ^{13}C shifts in alkylmercury compounds[44] and alkylindium(I) compounds,[45] and for ^{1}H shifts in organomercury hydrides[44]); and that (b) SO effects on the heavy atom itself (i.e., so-called ''heavy-atom effects on the heavy atom,'' HAHA[46]) may also be significant.

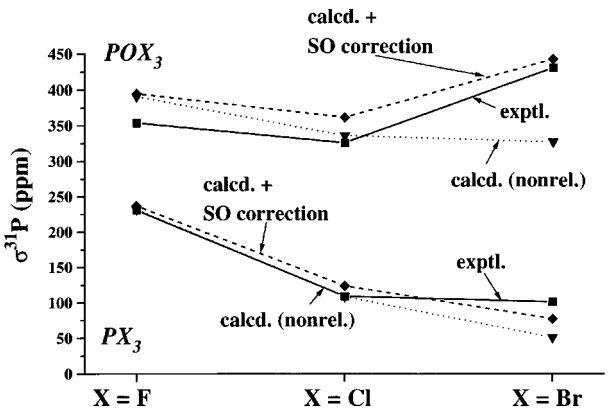

FIGURE 2. Absolute ^{31}P shielding constants for POX_3 and PX_3 molecules (X = F, Cl, Br). Calculations at the SOS-DFPT-IGLO level, using IGLO-II basis sets[2] on all atoms. Dotted lines refer to nonrelativistic calculations, dashed lines include one-electron SO corrections, solid lines give experimental[37] data. All other computational parameters are as in ref. 38. Experimental chemical shifts were converted to absolute shieldings, using a shielding value for 85% H_3PO_4 of 328.4 ppm (Jameson, C. J.; de Dios, A.; Jameson, A. K. Chem Phys Lett 1990, 167, 575).

Ligand Chemical Shifts in Transition-Metal Compounds

Ligands in the coordination sphere of transition metals are a special case of nuclei bonded to heavy atoms. The description of transition-metal compounds employing conventional *ab initio* methods usually requires highly sophisticated treatments of electron correlation. The more economic DFT-based approaches perform surprisingly well in the vast majority of cases and have opened the field of transition-metal chemistry to extensive and fruitful computational investigations. NMR properties appear to be no exception, and many DFT-based applications have been published addressing the chemical shifts of the metal nuclei as well as those of the ligands in their coordination sphere.[4] For the latter, scalar relativistic effects due to the neighboring metal have to be included. This has, up to now, been done either via appropriate ECPs or via the quasirelativistic frozen-core approximation (see earlier). There is not yet much explicit information on spin-orbit effects for such ligand shifts (except for some mercury compounds,[44] see earlier). There is some indirect evidence that SO contributions may become nonnegligible in the 5d series.[47,48] In any case, a large number of experimental ^{13}C, ^{17}O, ^{31}P, and ^{1}H chemical shifts (including principal components in some cases) have already been successfully reproduced for oxo,[5,28,29] carbonyl,[48–51] thiocarbonyl, carbyne, cyanide,[28] alkyl,[52] interstitial carbide,[53] olefin,[54,55] phosphine,[47,56] hydride,[57] and other ligands.[58] Beyond the detailed interpretation of the observed shield-

ing tensors, there have already been first attempts to use such computed ligand shifts in transition-metal complexes for structure determinations (see, e.g., ref. 52).

One quantity provided routinely by such calculations is the orientation of the shift tensor with respect to the molecular framework. This orientation contains important information on the electronic structure, but is very difficult to measure experimentally. How accurate are such shift-tensor orientations computed at the DFT level for transition-metal compounds? One of the very few single-crystal, solid-state NMR experiments available on a transition-metal cluster has been carried out by Eichele et al.[59] for the ^{31}P nucleus of the phosphinidene cluster $Ru_4(PPh)(CO)_{13}$. It is thus instructive to compute this shift tensor and its orientation with DFT methods.[58] Table I compares the shift tensor elements obtained at the SOS-DFPT-IGLO level to experiment. The agreement for δ_{11} and δ_{22} is good, but the computed δ_{33} is too large by ca. 75 ppm. It turns out that this discrepancy is due to problems with the localized orbitals underlying the IGLO approach (such problems have also been noted in other cases of transition-metal clusters with delocalized bonding[50]). A ''partial IGLO'' procedure, in which the highest 22 occupied (cluster-bonding) MOs are excluded from the localization procedure, gives significantly better agreement with experiment (last row in Table I). Irrespective of these different procedures, the computed orientation[58] of the shift tensor agrees to within better than 1° with experiment.[59] As shown in Figure 3, the largest component of the tensor, δ_{11}, is tilted by ca. 9° with respect to the phosphinidene P—C bond, whereas the experimental value is ca. 8° (with experimental error bars[60] of at least 2°). This indicates that such computed tensor orientations should be quite reliable and may thus be useful to relate the spectroscopic observables to the electronic structure of the system.

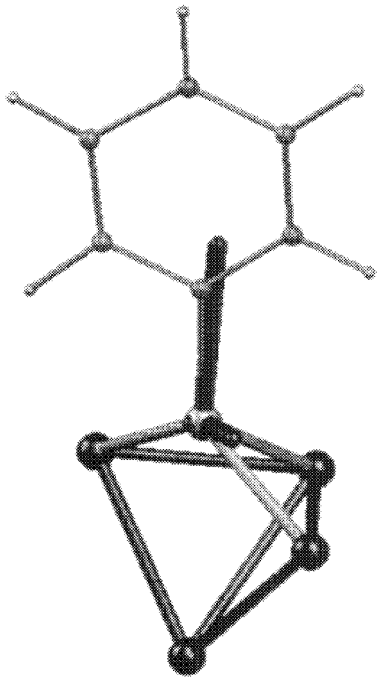

FIGURE 3. Computed orientation of the ^{31}P shift tensor in $Ru_4(PPh)(CO)_{13}$. Black sticks indicate the magnitude and orientation of the tensor components relative to the ball-and-stick framework of the cluster (carbonyl ligands were omitted).

Transition Metal Chemical Shifts

For the chemical shifts of the transition metals themselves, one might expect the importance of relativistic effects to increase with the atomic weight. In fact, quasirelativistic frozen-core UDFT-GIAO calculations of the absolute nuclear shield-

TABLE I.
Comparison of Experimental[59] and Computed[a] ^{31}P-Shift Tensors (in ppm with Respect to 85% H_3PO_4) for $Ru_4(PPh)(CO)_{13}$.

	δ_{11}	δ_{22}	δ_{33}	δ_{iso}
Exp.[59]	889	294	60	414
Calc. (full IGLO)[b]	923	328	135	462
Calc. (partial IGLO)[b]	848	282	65	398

[a] SOS-DFPT-IGLO calculations with PW91 functional. IGLO-II basis sets on P and the neighboring carbon atoms, quasirelativistic ECPs on Ru, and DZ basis sets on all other atoms.[58] Computed absolute shieldings have been converted to relative shifts using a shielding value for 85% H_3PO_4 of 328.4 ppm (from Jameson, C. J.; de Dios, A.; Jameson, A. K. Chem Phys Lett 1990, 167, 575).
[b] ''Full IGLO'' denotes a fully localized basis, whereas ''partial IGLO'' indicates that the 22 highest occupied MOs have been kept delocalized.

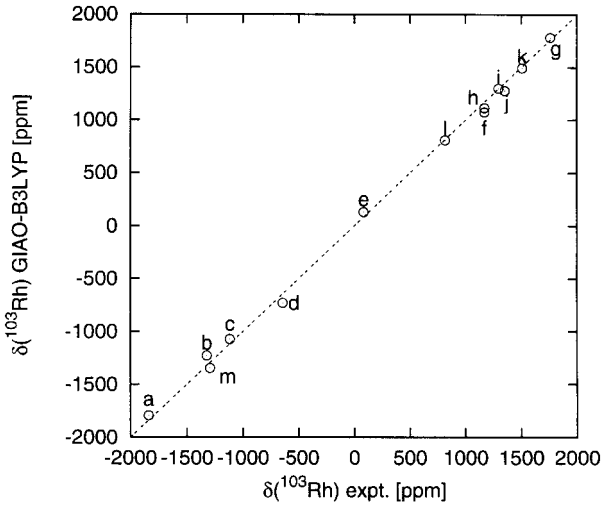

FIGURE 4. Computed (GIAO-B3LYP) vs. experimental ^{103}Rh chemical shifts for a larger set of compounds than studied previously (see ref. 64 for the set of compounds).

ings σ of MO_4^{2-} and $M(CO)_6$ (M = Cr, Mo, W) have indicated differences with respect to the corresponding nonrelativistic results[29]; these differences increase strongly as one goes down the triad (large relativistic effects on W and Hg shieldings have also been found in FPT–HF calculations[61]). When relative chemical shifts (δ) are considered (i.e., differences between absolute shieldings) these scalar relativistic effects are attenuated because the shielding contributions from the inner cores are quite similar in the various molecular environments and tend to cancel to a large extent in the δ values. Valence-shell contributions to σ are affected by relativity via the ''tails'' of the corresponding MOs that extend into the core region. The shape of such tails, and thus the relativistic effects on the valence-shell contribution to σ, may differ from one molecule to the other; that is, they may be much less transferable. At least for the 5d transition metals, relativistic effects on chemical shifts can be substantial—compare the nonrelativistic and relativistic $\delta(^{183}W)$ values of $W(CO)_6$ (relative to WO_4^{2-}), −4050 and −3615 ppm, respectively (experiment: −3505).[29] The corresponding values for $\delta(^{95}Mo)$ in $Mo(CO)_6$ are −1814 and −1804 ppm, respectively (experiment: −1857); here the effect is relatively small, certainly smaller than the shortcomings of the approximations inherent to DFT, particularly in the exchange-correlation functional. It thus appears that trends in chemical shifts of most 4d transition metals can be described at least qualitatively at a nonrelativistic level (provided no other, heavier atoms are present).

Support for this view comes from the good performance of the GIAO-B3LYP method for ^{103}Rh chemical shifts.[62] As is generally the case for transition-metal shifts, the choice of the exchange-correlation functional is critical. For a limited set of compounds, this particular hybrid functional has proven superior to ''pure DFT'' ones, which tend to underestimate substituent effects on $\delta(^{103}Rh)$.[63] Figure 4 illustrates that the performance of the GIAO–B3LYP method persists when applied to a somewhat larger, more diverse set of Rh compounds.[64] It should be noted that, in the Gaussian-94 implementation,[22] CHF-type coupling terms are included proportionally for that part of the exchange potential, which has been replaced by Hartree–Fock exchange (see earlier).

The B3LYP functional has also been applied successfully to ^{57}Fe and ^{59}Co chemical shifts,[62,65,66] both of which are tremendously underestimated with ''pure'' gradient-corrected density functionals.[67,68] The ^{57}Fe chemical shift of ferrocene, a particularly challenging case for pure DFT methods,[67] is well reproduced with the GIAO-B3LYP method[62]; at the same level, even the absolute cobalt shieldings of $Co(CN)_6^{3-}$ and $Co(acac)_3$, as well as the Co—C bond-length-shielding derivative for $Co(CN)_6^{3-}$ have been found quite close to the corresponding experimental estimates.[66] GIAO-B3LYP ^{57}Fe chemical shifts computed for model compounds for iron-containing porphyrins and proteins have been found in moderate accord with the actual experimental data, extending the range of $\delta(^{57}Fe)$ values recovered in the calculations to more than 12,000 ppm.[65] The computed shifts are very sensitive to structural details (e.g., poor accord with experiment is obtained when the structures of the models are based on ''distorted'' solid-state arrangements). Refinements of key structural parameters are thus foreseeable in the near future, where the degree of agreement between theoretical and experimental chemical shifts (and/or other observables) is optimized with respect to these parameters.[69] In fact, such a structural application has recently been reported for the Fe—CO bending angle in CO myoglobin.[65b]

The first DFT-based computation of transition-metal chemical shifts had been reported for some vanadium compounds.[24] A recent systematic study has shown that substituent effects on $\delta(^{51}V)$ are similarly well reproduced with pure DFT methods and with the B3LYP functional.[70] The former and

latter tend to under- and overestimate the chemical shifts somewhat, respectively, but trends are very well described in a qualitative fashion. One such trend that may be of practical use has been predicted computationally[71]: It has been shown that, in oxovanadium(V)–Lewis-acid adducts $Me_3V{=}O \cdots X$, the $\delta(^{51}V)$ value increases with the Lewis-acid strength of X. In the same sequence, the barrier for ethylene insertion into a V—C bond decreases. Figure 5 illustrates the correlation between these two properties. Transferred to a real, ethylene-polymerizing catalyst, $(Me_3\delta iCH_2)_3V{=}O \cdots Al(CH_2\delta iMe_3)_3$, these results indicate that the catalytic activity should increase with the strength of the Lewis acid. Furthermore, a screening of the latter should be possible using ^{51}V NMR: the complexes with the most deshielded ^{51}V nucleus should also be the most active catalysts.

For most of the transition-metal chemical shifts studied so far, the B3LYP hybrid functional performs similar or better than pure density functionals. The latter seem to underestimate proportionally the paramagnetic contributions, σ_P, which is apparently corrected for by inclusion of some Hartree–Fock exchange, and of the corresponding CHF-type coupling terms (see earlier), in the hybrid functional [note that, in the case of $\delta(^{103}Rh)$, pure HF methods significantly overestimate the chemical shifts[63]]. It has yet to be elucidated if the good performance of hybrid functionals is a manifestation of the physical reasoning put forward to motivate the inclusion of HF exchange in density

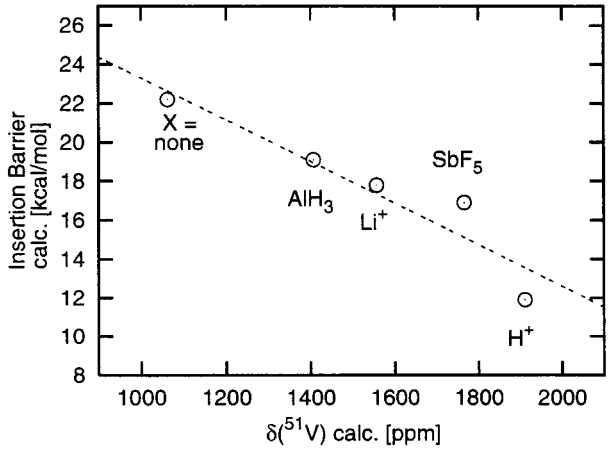

FIGURE 5. Predicted correlation between olefin-insertion barriers (i.e. catalytic activities) and ^{51}V chemical shifts for $R_3V{=}O \cdots X$ Lewis-acid complexes (calculated for R = Me); from ref. 71.

functionals,[72] or simply the result of fortunate error compensation. In any case, the GIAO–B3LYP scheme is not a panacea, as evidenced by the $\delta(^{95}Mo)$ results displayed in Figure 6: For the specific set of Mo compounds studied,[73] the "pure" DFT method UDFT-GIAO-BPW91 affords a good description of the substituent effects on $\delta(^{95}Mo)$ (Fig. 6a; the slope of calc. vs. exp. shifts is close to unity). Inclusion of Hartree–Fock exchange now results in a severe overestimation of the chemical-shift trends (Fig. 6b; the corresponding slope is much larger than unity). Furthermore, compounds involving (Mo, Mo) multiple bonds show large additional deviations from the experimental δ values, with errors up to 1800 ppm for $Mo_2(O_2CR)_4$. Apparently, the electronic structure of these molecules is so poorly described at the HF level that partial incorporation of HF exchange causes the DFT-computed magnetic shieldings to deteriorate dramatically. A similar overshooting of the paramagnetic contributions by hybrid functionals has been found for ^{17}O shifts in transition-metal oxo complexes.[5]

Improved functionals *without* exchange mixing would of course be desirable. The design of new exchange and correlation functionals is a very active field, and so there is some hope that better functionals will eventually become available. Recently, Adamson et al. proposed "empirical density functionals" composed of suitable linear combinations of modified Becke-type exchange functionals.[74] The parameters were fitted such that experimental heats of formations were well reproduced for a large set of small molecules (containing mostly only light atoms), using moderate 6-31 + G* basis sets.[74] The quality of thermochemical data computed with such modified functionals was comparable to those obtained with hybrid functionals like B3LYP, without the need to include Hartree–Fock exchange terms. We have now implemented the "double-Becke" exchange functional of Adamson et al. in the deMon–KS code and tested its performance for transition-metal chemical shifts. Table II compares computed ^{57}Fe shifts for a variety of species obtained with this "double-Becke" functional (employing the P86 instead of the LYP correlation functional used by Adamson et al.[74]; thus, the abbreviation DBP86) to results obtained with other functionals. Although the agreement with experimental shifts is improved slightly, compared with the "standard" gradient-corrected BP86 and PW91 functionals, the

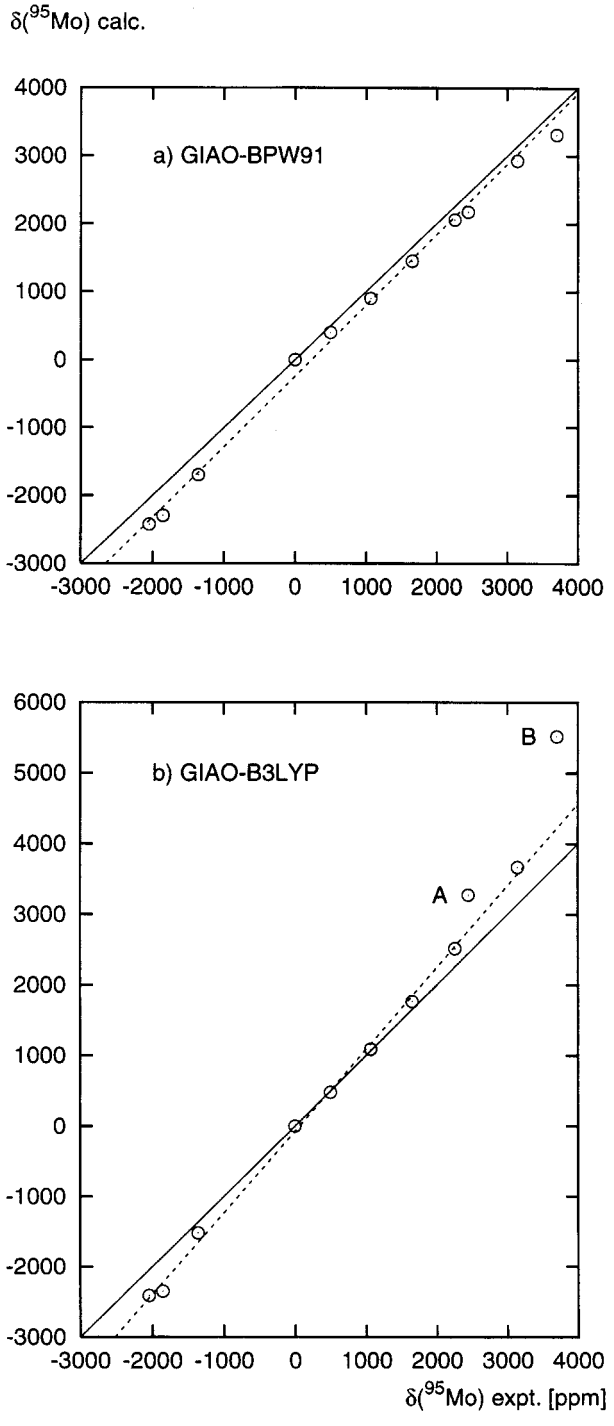

FIGURE 6. Computed vs. experimental ^{95}Mo chemical shifts (in ppm) relative to MoO_4^{2-} (see ref. 73 for the set of compounds); entries for species involving (Mo, Mo) multiple bonds: $Mo_2(OR)_6$ (A); $Mo_2(O_2CR)_4$ (B).

results are clearly still much poorer than those obtained with the hybrid B3LYP functional. Additional tests show that omission of the SOS-DFPT correction terms (i.e., using the UDFT approach) lead to changes in absolute shieldings of ca. 100–300 ppm. However, most of the relative shifts are much less affected.

Thus, one is left with the somewhat unsatisfying conclusion that, in contrast to the situation for chemical shifts of main group nuclei (including ligand chemical shifts in transition-metal compounds), any particular DFT method employed for transition-metal chemical-shift calculations has to be carefully reassessed for every new problem at hand, at least until better functionals (i.e., closer to the elusive, universal one) become available. Most likely, the large sensitivity of the metal shifts to the exchange-correlation potential is related to the largely local types of electronic excitations involved. These are known to be very poorly described by most functionals currently available.[75] This situation, however, does not preclude chemically relevant applications of chemical-shift calculations for this important class of compounds.

Large Molecules

As molecules of interest become larger, the computational expense for property evaluations increases sharply. Reflecting the growing importance of life sciences, applications of chemical-shift calculations to biomolecules are emerging rapidly. Only a few of these applications will be highlighted here; the remainder of the section will deal with recent results for another class of large molecules, the fullerenes.

UDFT-GIAO-BLYP ^{13}C and ^{15}N chemical shifts have recently been reported for two chlorophylls, including bacteriochlorophyll *a*, which consists of 140 atoms (more than 60 nonhydrogen atoms).[76] Although the theoretical $\delta(^{15}N)$ values are not in good accord with experiment, probably due to the small basis set and neglect of medium effects, the $\delta(^{13}C)$ data are described well and can be used to suggest revisions of the original assignments.

Much effort has been spent on the theoretical description of the chemical shifts of proteins. The particular chemical shifts of a given residue are primarily governed by the conformations along the peptide chain and, to a lesser extent, by the orientations of flexible side chains. When the ^{13}C chemi-

TABLE II.
^{57}Fe Chemical Shifts[a] Computed with Various Density Functionals.

Molecule	SOS-DFPT-PW91[b]	SOS-DFPT-BP86[c]	SOS-DFPT-DBP86[d]	UDFT-GIAO-B3LYP[b]	Experiment
$Fe(CO)_3$(*cyclo*-C_4H_4)	−445	−444	−424	−504	−538
$Fe(CO)_5$	0	0	0	0	0
$Fe(CO)_3(H_2C{=}CHCH{=}CH_2)$	−113	−123	−102	32	4
$Fe(CO)_4(H_2C{=}CHCN)$	102	90	104	210	303
$Fe(CO)_3(H_2C{=}CHCH{=}O)$	627	629	664	1237	1274
$Fe(C_5H_5)_2$	156	166	251	1485	1532

[a] Relative to $Fe(CO)_5$ using the same structures and basis II as detailed in ref. 62; absolute shieldings, SOS-DFPT-PW91—1529, SOS-DFPT-BP86—1618, SOS-DFPT-DBP86—1571, UDFT-GIAO-B3LYP—2903 ppm.
[b] Taken from ref. 62.
[b] Becke's 1988 exchange functional (Becke, A. D. Phys Rev A 1988, 38, 3098) with Perdew's 1986 correlation functional (Perdew, J. P. Phys Rev B 1986, 33, 8822).
[d] Empirical gradient-corrected functional analogous to that of Adamson et al.[74] based on the ''double-Becke-type'' exchange part, but using the P86 instead of the LYP correlation functional.

cal shifts (C^{α}, C^{β}, and C^{γ}), computed for a ''protected'' valine molecule (N-formylvaline amide) using parameters from X-ray structures of large proteins, are compared with the experimental $\delta(^{13}C)$ solution data of the corresponding residues, the results obtained with DFT methods are far superior to those obtained at the uncorrelated HF-GIAO level.[77] In addition, partial structure optimization of the valine side chains further improves the accord between theoretical and experimental chemical shifts. A method has recently been devised to derive structural data for proteins or polypeptides from their NMR spectra: From the experimental chemical shifts, together with the computed chemical-shift surfaces of the individual amino acid residues (suitably ''protected''), the approximate torsional angles about the peptide links in the protein and, thus its secondary structure, can be deduced via a Bayesian probability (''Z-surface'') approach.[78] It can be anticipated that the reliability of this approach will be further improved by using more accurate, theoretical chemical-shift surfaces; for instance, those obtained from DFT-based methods. Such DFT computations may also be used together with thermal averaging in the case of flat potential surfaces and/or many low-lying conformers (see ref. 79 for a recent study of hydrocarbon compounds).

Fullerenes are another class of compounds, the sheer sizes of which pose a challenge to extensive first-principles treatments. Relative chemical shifts appear to be reasonably well described already at the Hartree–Fock level.[80] To our knowledge, no electron-correlated chemical-shift calculations have yet been reported for fullerenes. It is therefore instructive to inspect the preliminary DFT results in Tables III and IV.[81]

For the ^{13}C chemical shifts of C_{60} and C_{70}, indeed only minor changes are found in going from HF-GIAO to UDFT-GIAO-BPW91 (Table III). The choice of the standard is important,[80b,c] as can be seen for C_{70}, where theoretical and experimental shifts agree much better when referenced to C_{60} (see values in parentheses).

For a given fullerene or a derivative thereof, not only the $\delta(^{13}C)$ values are of interest; but also the endohedral chemical shift at the very center of the cage. The latter are accessible experimentally via the ^{3}He chemical shifts of the corresponding endohedral He-fullerene compounds.[82] In general, experimental data can be reproduced at the HF-GIAO level within ca. 2–3 ppm, with a slight tendency to overestimate the endohedral shieldings (see, e.g., ref. 81b and references cited therein). Electron-correlation effects, as assessed by the UDFT–GIAO–BPW91 vs. HF–GIAO results in Table IV, are indeed indicated to reduce the computed shieldings. These effects can be quite small (less than 1 ppm, C_{70}) or very large (almost 20 ppm, C_{60}^{6-}), and the DFT results are usually closer to experiment. For instance, one of the two signals around ca. −8 ppm seen experimentally for He at $C_{60}H_{36}$[83a] may well be due to the most stable isomer of T symmetry: the initially predicted HF-GIAO endohedral shift around −11 ppm[83b] is reduced to ca. −9 ppm at the DFT level (Table IV). The second isomer could be the C_3 form suggested recently for

TABLE III.
^{13}C[a] Chemical Shifts of C_{60} and C_{70}, Computed with GIAO Method, DZP Basis Set, and MP2/TZP and BP86/TZP Structures, Respectively.

Molecule	Nucleus[b]	HF-GIAO	UDFT-GIAO-BPW91	Experiment[c]
C_{60}	C	149.0 (0.0)	144.2 (0.0)	142.7 (0.0)
C_{70}	C(a)	155.5 (6.0)	152.6 (8.4)	150.1 (7.4)
	C(b)	151.9 (2.9)	148.1 (3.9)	146.8 (4.1)
	C(c)	152.3 (3.3)	149.5 (5.3)	147.5 (4.8)
	C(d)	150.1 (1.1)	147.5 (3.3)	144.8 (2.1)
	C(e)	139.0 (−10.0)	131.4 (−12.8)	130.3 (−12.4)

[a] Relative to TMS (benzene, in the corresponding structure used as primary reference; absolute shieldings, HF-GIAO//MP2—68.1, UDFT-GIAO-BPW91//MP2—66.0, HF-GIAO//BP86—66.3, UDFT-GIAO-BPW91//BP86—64.5 ppm; converted to the TMS scale using the experimental ^{13}C chemical shift of benzene, 128.5 ppm); in parentheses: relative to C_{60}. [b] Labels (a)–(e) denote layers from the pole to the equator in C_{70}. [c] From Taylor, R.; Hare, J. P.; Abdul-Sala, A. K.; Kroto, H. W. J Chem Soc Chem Commun 1990, 1423.

the analogous $C_{60}F_{36}$ system,[83c] rather than the D_{3d} form speculated previously.[83a]

Unfortunately, the endohedral chemical shift of the most important fullerene, C_{60}, appears to be a problem case for DFT: a substantial deshielding of 10 ppm is computed in going from HF-GIAO to UDFT-GIAO-BPW91 (Table III), resulting in a large deviation from experiment for the latter. The individual ring currents (as assessed[81b] by NICS[84] calculations) have much more paratropic character at the DFT level, at which the diatropic currents in the six-membered rings have practically vanished. Practically the same result is obtained with the hybrid B3LYP functional (endohedral shift +1.0 ppm) instead of the BPW91 one. Ring-current effects in fullerenes may thus be quite sensitive to electron correlation; further theoretical work in this area is desirable.

In conclusion, chemical shifts of relatively large molecular systems can now be computed with available DFT-based methods. The usual scaling properties with system size of first-principle methods eventually puts limits to the size of molecules that can be treated. However, continuing developments of theoretical methods, efficient implementations, and computer hardware are expected to further expand these limits.

TABLE IV.
Endohedral Chemical Shifts[a] of Fullerenes and Fullerene Derivatives, Computed with the GIAO Method and DZP Basis Set.

Molecule	HF-GIAO	UDFT-GIAO-BPW91	Experiment[b]
C_{60}[c]	−8.5	1.5	−6.3[d]
C_{70}[e]	−29.3	−28.7	−28.8[d]
C_{60}^{6-}[f]	−66.5	−47.4	−49[g]
$C_{60}H_{36}$ T[h]	−10.6	−8.8	−7.7/−7.8[i]
$C_{60}H_{36}$ $C_3(3)$[h]	−8.5	−7.0	″
$C_{60}H_{36}$ $D_{3d}(2)$[h]	−7.7	−6.1	″

[a] At the center of mass of each cage (in ppm); variations of the computed values up to 1 Å around the center are very small for fullerenes (0.1 ppm) and are slightly larger for the $C_{60}H_{36}$ isomers (ca. 1 ppm). [b] $\delta(^3He)$ of the corresponding endohedral He compound. [c] MP2/TZP structure. [d] Ref. 82. [e] BP86/TZP structure. [f] HF/6-31 + G structure. [g] M. Rabinovitz, unpublished (communicated in a lecture given 1997 in Zürich). [h] HF/3-21G structure. [i] Ref. 83a.

Weakly Bound Systems: Shielding Tensor Calculations for Ne_2 as a Function of Ne—Ne Distance

Are present DFT methods able to describe weak interactions properly? This question is of fundamental interest and remains topical (see, e.g., ref. 85 and references therein). For rare-gas dimers, typical systems studied in that respect, different exchange-correlation functionals give very different results, ranging from unbound complexes (Becke88) to a significant overbinding with the VWN functional. Thus, van der Waals bonding is obviously not well described by the present DFT-based methods, and this class of compounds is widely regarded as a challenge for DFT. It is of interest to determine whether this also holds true for the computed shielding tensors.

For the present study we have chosen the Ne_2 molecule, and we have performed calculations of the shielding tensor as a function of the Ne—Ne distance with different combinations of density functionals (VWN, BPW91, BLYP, B3LYP) and with HF and CCSD(T) methods. All calculations were carried out with Dunning's correlation-consistent cc-PVTZ basis,[86] using the GIAO approach and employing the Gaussian-94[87] (DFT and HF calculations) and ACES[88] [CCSD(T)] programs. The results for the isotropic Ne shielding σ and for the anisotropy $\Delta\sigma$ are presented in Figures 7 and 8, respectively.

For the isotropic shieldings, all the theoretical data, except for those obtained with the VWN functional, are very close to the CCSD(T) results, which are considered as a benchmark in the present study (Fig. 7). At the local VWN level, larger deviations from the CCSD(T) σ values are apparent, but the overall trend with the Ne—Ne distance is basically the same. The major error is associated with a wrong limit, namely the shielding of the free Ne atom. The apparent shortcomings of this functional are thus due to the description of an atom, not the interaction between two atoms! All other, gradient-corrected functionals of this study perform quite well, affording σ values in good accord with the CCSD(T) data over a large range of Ne—Ne separations. Because σ is underestimated with the ''pure'' density functionals, and overestimated at the HF level, the hybrid B3LYP functional performs best. Remarkably, all local and nonlocal exchange-correlation functionals employed reproduce the shape of the CCSD(T) shielding function correctly, giving a maximum at about 3.2 Å (this exceeds the asymptotic value slightly, by about 0.02–0.03 ppm). At shorter distances,

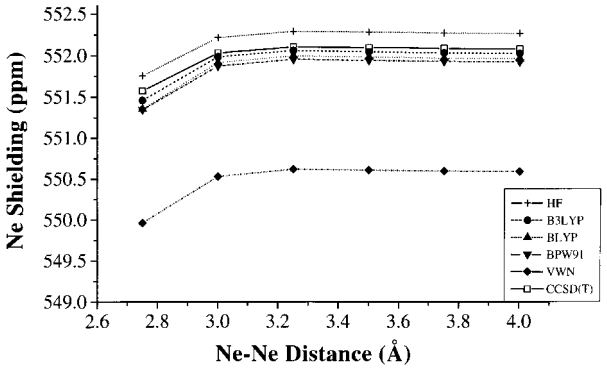

FIGURE 7. Isotropic Ne shielding σ in Ne_2 as a function of the Ne—Ne distance, computed using various *ab initio* and DFT methods.

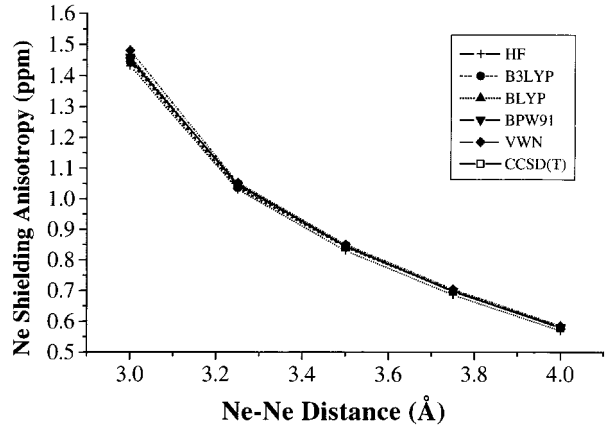

FIGURE 8. Ne shielding anisotropy $\Delta\sigma$ in Ne_2 as a function of the Ne—Ne distance, computed using various *ab initio* and DFT methods.

differences between the DFT and CCSD(T) values appear to increase somewhat, but the interaction in that region is certainly not a weak one any more.

The shielding anisotropies often provide a more stringent test to the reliability of a particular method than the isotropic shieldings themselves. All methods used in this study, however, afford practically the same results for $\Delta\sigma$ as a function of the Ne—Ne distance (Fig. 8). The variation in the isotropic shielding from one method to the other is therefore due to a simultaneous shift of both principal components. This shift may be related to the inaccurate asymptotic behavior (i.e., the error for the Ne atom with the VWN method), rather than with the description of the weak interaction itself. The effect of the latter on the shielding appears rather undemanding with respect to the theoretical level, at least for Ne_2. Therefore, the limiting factor for DFT-computed chemical shifts in weakly bound systems will most likely be the quality of the structure (in particular, when obtained from optimizations), rather than the chemical-shift calculation itself.

Summary

Both theoretical developments and chemical applications of DFT-based chemical-shift calculations are blossoming, and are continuously expanding the limits on classes and size of compounds that can be studied computationally. As could be illustrated by selected examples, a broad spectrum of applications is emerging; for instance, in organo-

metallic chemistry, in homogeneous catalysis, or in bioinorganic chemistry. In conjunction with available experimental NMR data, theoretical results can already afford reliable information regarding the structures of products and reactive intermediates present in the experiments. Numerical predictions are being made that may help to design new experiments for very practical purposes, such as a potential speed-up of catalytic reactions. On a more fundamental level, theoretical computations are giving insights into the underlying mechanisms that determine the observed NMR properties, affording an invaluable interpretative tool. New or newly discovered concepts can be formulated or substantiated, such as the analogy between spin–orbit effects on chemical shifts and spin–spin coupling constants.

For all these purposes, the chemical-shift calculations need to be performed at sufficiently high levels of sophistication. Whereas the present density-functional methods cannot yet match the accuracy of the most sophisticated *ab initio* approaches, they outperform the uncorrelated coupled-Hartree–Fock variants. For some time to come, DFT-based methods will be the key to the study of NMR properties for transition-metal compounds, as no other quantum-chemical method presently available allows for the necessary inclusion of electron correlation at manageable computational cost. There are problem cases, however, such as certain transition-metal chemical shifts, which leave room for further improvement, primarily concerning the development of better exchange-correlation functionals. At least in these problem cases, not all functionals designed to reproduce experimental thermochemical data appear to be equally well suited for chemical-shift computations.

Notable progress is being made regarding the inclusion of relativistic effects in the calculations. It is now possible to account, at least in preliminary implementations, for electron-correlation, scalar relativistic effects, and spin–orbit coupling at the same time, allowing accurate chemical-shift computations for a vast number of compounds containing heavy elements, including transition metals. For the NMR properties of the latter, fully relativistic approaches will probably also have to include relativistic hyperfine operators.[89]

Spin–spin coupling constants, mentioned only briefly in the present article, turn out to be even more demanding with respect to basis set, level of electron-correlation treatment, or exchange-correlation functionals employed. Nevertheless, similar progress, like that for chemical shifts, is being made for the DFT-based calculations of this property.[4] Thus, the ''DFT route to NMR spectra'' is already open.

Acknowledgments

M. B. thanks Prof. W. Thiel for his continuous support. Permission of Dr. W. Leitner to make use of unpublished experimental data is acknowledged. Calculations in Zürich were performed on a Silicon Graphics PowerChallenge and on IBM RS6000 workstations at the university and at the ETH (C4 cluster). V. G. M. thanks the Alexander von Humboldt Stiftung for the donation of a HP9000/C160 workstation.

References

1. Tossell, J. A. (Ed.) Nuclear Magnetic Shieldings and Molecular Structure; Kluwer: Dordrecht, 1993.
2. Kutzelnigg, W.; Fleischer, U.; Schindler, M. NMR—Basic Principles and Press, Vol. 23; Springer: Heidelberg, 1990; pp. 165–262.
3. See, e.g., (a) Gauss, J.; Stanton, J. F. Chem Phys 1996, 104, 2574; (b) van Wüllen, C.; Kutzelnigg, W. J Chem Phys 1996, 104, 2330, and references cited therein.
4. Kaupp, M.; Malkin, V. G.; Malkina, O. L. In P. v. R. Schleyer (Ed.) Encyclopedia of Computational Chemistry; Wiley: New York, 1998.
5. Kaupp, M.; Malkina, O. L.; Malkin, V. G. J Chem Phys 1997, 106, 9201.
6. Schreckenbach, G.; Ziegler, T. Theor Chem Acc 1998, 2, 71.
7. See, e.g., Ziegler, T. Chem Rev 1991, 91, 651.
8. Rajagopal, A. K.; Callaway, J. Phys Rev B 1973, 7, 1912.
9. Vignale, G.; Rasolt, M. Phys Rev B 1988, 37, 10685.
10. Lee, A. M.; Handy, N. C.; Colwell, S. M. J Chem Phys 1995, 103, 10095.
11. Lee et al. used a local-density-type approximation for the current dependency.
12. A gradient-corrected current-density functional has recently been suggested: Becke, A. D. Can J Chem 1996, 74, 995.
13. Capelle, K.; Gross, E. K. U. Phys Rev Lett 1997, 78, 1872.
14. van Wüllen, C. J Chem Phys 1995, 102, 2806; See also: Malkin, V. G.; Malkina, O. L.; Salahub, D. R. J Chem Phys 1996, 104, 1163; van Wüllen, C. J Chem Phys 1996, 104, 1164.
15. A ''magnetic-field'' DFT approach has been suggested by Harris et al. (see, e.g., Salsbury, Jr., F. R.; Harris, R. A. Chem Phys Lett 1997, 279, 247, and references therein), but this method does not yet appear to provide a scheme for calculations of useful accuracy).
16. The most important difference comes from the vacant orbitals, which experience an effective potential due to $n - 1$ electrons within the Kohn–Sham method, but due to n electrons within the Hartree–Fock scheme.[24]

17. It appears possible to prove rigorously the special properties of the Kohn–Sham Hamiltonian as a basis for perturbation theories (B. Farid, unpublished results, personal communication to M. K.). See also: Farid, B. Philos Mag B 1997, 76, 145.
18. See, e.g., Bieger, W.; Seifert, G.; Eschrig, H.; Grossman, G. Chem Phys Lett 1985, 115, 275; Malkin, V. G.; Zhidomirov, G. M. Zh Strukt Khim 1988, 29, 32; Freier, D. A.; Fenske, R. F.; Xiao-Zeng, Y. J Chem Phys 1985, 83, 3526; Friedrich, K.; Seifert, G.; Grossmann, G. Z Phys D 1990, 17, 45.
19. Malkin, V. G.; Malkina, O. L.; Salahub, D. R. Chem Phys Lett 1993, 204, 80; Chem Phys Lett 1993, 204, 87.
20. Schreckenbach, G.; Ziegler, T. J Phys Chem 1995, 99, 606.
21. Rauhut, G.; Puyear, S.; Wolinski, K.; Pulay, P. J Phys Chem 1996, 100, 6310.
22. Cheesemann, J. R.; Trucks, G. W.; Keith, T. A.; Frisch, M. J. J Chem Phys 1996, 104, 5497.
23. Ardvengo, A. J.; Dixon, D. A.; Kumashiro, K. K.; Lee, C.; Power, W. P.; Zilan, K. J Am Chem Soc 1994, 116, 6361.
24. Malkin, V. G.; Malkina, O. L. Casida, M. E.; Salahub, D. R. J Am Chem Soc 1984, 116, 5898.
25. Malkin, V. G.; Malkina, O. L.; Eriksson, L. A.; Salahub, D. R. In J. Seminario and P. Politzer (Eds.) Modern Density Functional Theory: A Tool for Chemistry; Theoretical and Computational Chemistry, Vol. 2; Elsevier: Amsterdam, 1995; pp. 273–347.
26. See, e.g., Pyykkö, P. Chem Rev 1988, 88, 563.
27. Kaupp, M.; Malkin, V. G.; Malkina, O. L.; Salahub, D. R. J Am Chem Soc 1995, 117, 1851; J Am Chem Soc 1995, 117, 8492.
28. Kaupp, M.; Malkin, V. G.; Malkina, O. L.; Salahub, D. R. Chem Phys Lett 1995, 235, 382.
29. Schreckenbach, G.; Ziegler, T. Int J Quantum Chem 1997, 61, 899.
30. Ballard, C. C.; Hada, M.; Kaneko, H.; Nakatsuji, H. Chem Phys Lett 1996, 254, 170.
31. Ishikawa, Y.; Nakajima, T.; Hada, M.; Nakatsuji, H. Chem Phys Lett 1998, 283, 119.
32. For recent applications of the ZORA approach to ESR parameters, see: van Lenthe, E.; van der Avoird, A.; Wormer, P. E. S. J Chem Phys 1998, 108, 4783.
33. Kaupp, M.; Malkina, O. L.; Malkin, V. G.; Pyykkö, P. Chem Eur J 1998, 4, 118.
34. Malkin, V. G.; Malkina, O. L.; Salahub, D. R. Chem Phys Lett 1996, 261, 335.
35. Malkin, V. G.; Malkina, O. L.; Salahub, D. R. Chem Phys Lett 1994, 221, 91; Malkina, O. L.; Salahub, D. R.; Malkin, V. G. J Chem Phys 1996, 105, 8793.
36. Nomura, Y.; Takeuchi, Y.; Nakagawa, N. Tetrahedron Lett 1969, 8, 639.
37. See, e.g., Mason, J. (Ed.) Multinuclear NMR; Plenum: New York, 1987, and references cited therein.
38. Kaupp, M.; Malkina, O. L.; Malkin, V. G. Chem Phys Lett 1997, 265, 55.
39. Duchâteau, M. Dissertation, Universität Dortmund, 1994; Duchâteau, M.; Keller, H. L. Z Allg Anorg Chem (in press); H. L. Keller, personal communication to M. K.
40. See e.g., Ecker, A.; Üffing, C.; Schnöckel, H. Z Allg Anorg Chem 1998, 624, 817.
41. Nakatsuji, H.; Hu, Z.-M.; Nakajima, T. Chem Phys Lett 1997, 275, 429.
42. Kaupp, M.; Malkina, O. L.; Malkin, V. G.; Pyykkö, P. Presented as a poster at the Ninth International Congress of Quantum Chemistry, Atlanta, GA, 1997.
43. Pregosin, P. S. (Ed.) Transition Metal Magnetic Resonance; Elsevier: Amsterdam, 1991.
44. Kaupp, M.; Malkina, O. L. J Chem Phys 1998, 108, 3648.
45. Uhl, W.; Jantschak, A.; Saak, W.; Kaupp, M.; Wartchow, R. Organometallics (in press).
46. Edlund, U.; Lejon, T.; Pyykkö, P.; Venkatachalam, T. K.; Buncel, E. J Am Chem Soc 1987, 109, 5982.
47. Kaupp, M. Chem Ber 1996, 129, 535.
48. Kaupp, M. Chem Eur J 1996, 2, 348.
49. Kaupp, M.; Malkin, V. G.; Malkina, O. L.; Salahub, D. R. Chem Eur J 1996, 2, 24.
50. Salzmann, R.; Kaupp, M.; McMahon, M.; Oldfield, E. J Am Chem Soc 1998, 120, 4771.
51. (a) Ruiz-Morales, Y.; Schreckenbach, G.; Ziegler, T. J Phys Chem Soc 1996, 100, 3359; (b) Ehlers, A. W.; Ruiz-Morales, Y.; Baerends, E. J.; Ziegler, T. Inorg Chem 1997, 36, 5031.
52. Kaupp, M. J Am Chem Soc 1996, 118, 3018.
53. Kaupp, M. J Chem Soc Chem Commun 1996, 1141.
54. Havlin, R.; McMahon, M.; Srinivasan, R.; Le, H.; Oldfield, E. J Phys Chem A 1997, 101, 8908.
55. Bernard, G. M.; Wu, G.; Wasylishen, R. E. J Phys Chem A 1998, 102, 3184.
56. Ruiz-Morales, Y.; Ziegler, T. J Phys Chem A 1998, 102, 3970.
57. Ruiz-Morales, Y.; Schreckenbach, G.; Ziegler, T. Organometallics 1996, 15, 3920.
58. Kaupp, M. Habilitationsschrift, Universität Stuttgart, Stuttgart, Germany, 1996.
59. Eichele, K.; Wasylishen, R. E.; Corrigan, J. F.; Taylor, N. J.; Carthy, A. J. J Am Chem Soc 1995, 117, 6961.
60. Eichele, K. Personal communication to M. K.
61. Nakatsuji, H.; Hada, M.; Kaneko, H.; Ballard, C. C. Chem Phys Lett 1996, 255, 195; Hada, M.; Nakatsuji, H.; Kaneko, H.; Ballard, C. C. Chem Phys Lett 1996, 261, 7.
62. Bühl, M. Chem Phys Lett 1997, 267, 251.
63. Bühl, M. Organometallics 1997, 16, 261.
64. Bühl, M. To be published. The same methods and basis sets as described in ref. 62 have been employed [compounds a–g: $RhCp_2^+$, $RhCp(CO)_2$, $Rh(CO)_2(C_5H_4NO_2)$, $Rh(CO)_4^-$, $RhCl_2(CO)_2^-$, $Rh(acac)(C_2H_4)_2$, Rh(acac)(COT)]. Compounds h—m: $Rh(acac)(C_2H_4)(C_2F_4)$ (h), Rh(acac)(COD) (i), $Rh(acac)(C_2H_4)(cis\text{-}C_4H_8)$ (j), $Rh(acac)(cis\text{-}C_4H_8)_2$ (k), $Rh(bipy)(COD)^+$ (l), $Rh(Me_2PCH_2CH_2PMe_2)_2^+$ (m); experimental data from: (a) Mann, B. E. In P. S. Pregosin (Ed.), Transition Metal NMR; Elsevier: Amsterdam, 1991; p. 177; (b) Akermark, B.; Blomberg, M. A.; Glaser, J.; Öhrstrom, L.; Wahlberg, S.; Wärnmark, K.; Zetterberg, K. J Am Chem Soc 1994, 116, 3405; (c) Leitner, W.; Bühl, M.; Fornika, R.; Six, C.; Baumann, W.; Dingus, E.; Kessler, M.; Krueger, C.; Rufinska, A. Manuscript submitted.
65. (a) Godbout, N.; Havlin, R.; Salzmann, R.; Debrunner, P. G.; Oldfield, E. J Phys Chem A 1998, 102, 2342; (b) McMahon, M. C.; deDios, A. C.; Godbout, N.; Salzmann, R.; Laws, D. D.; Le, H.; Havlin, R. H.; Oldfield, E. J Am Chem Soc 1998, 120, 4784.
66. Godbout, N.; Oldfield, E. J Am Chem Soc 1997, 119, 8065.

67. Bühl, M.; Malkina, O. L.; Malkin, V. G. Helv Chim Acta 1996, 79, 742.
68. Chan, C. C. J.; Au-Yeung, S. C. F.; Wilson, P. J.; Webb, G. A. J Mol Struct 1996, 365, 125.
69. For a review of structural applications of chemical-shift calculations see: Bühl, M. In P. v. R. Schleyer (Ed.) Encyclopedia of Computational Chemistry; Wiley: New York 1998.
70. Bühl, M.; Hamprecht, F. A. J Comput Chem 1998, 19, 113.
71. Bühl, M. Angew Chem Int Ed 1998, 37, 142.
72. Becke, A. D. J Chem Phys 1993, 98, 5648.
73. Bühl, M. To be published. Methods and basis sets corresponding to those of ref. 62 have been employed for the following molecules: MoO_4^{2-}, MoO_3S^{2-}, $MoO_2S_2^{2-}$, $MoOS_3^{2-}$, MoS_4^{2}, $MoSe_4^{2-}$, $Mo(CO)_6$, $Mo(C_6H_6)_2$, $Mo(Cp)(CO)_3H$, $Mo_2(O_2CR)_4$ (calc. R = H, exp. R = Me), $Mo_2(OR)_6$ (calc. R = H, exp. R = CH_2CMe_3); experimental data from: Minelli, M.; Enemark, J. H.; Brownlee, R. T. C.; O'Connor, M. J.; Wedd, A. G. Coord Chem Rev 1985, 68, 169.
74. Adamson, R. D.; Gill, P. M. W.; Pople, J. A. Chem Phys Lett 1998, 284, 6.
75. See, e.g., (a) Ziegler, T.; Li, J. Can J Chem 1993, 72, 783; (b) Fournier, R.; J Chem Phys 1993, 99, 1801; (c) Holthausen, M. C.; Heinemann, C.; Cornehl, H. H.; Koch, W.; Schwarz, H. J Chem Phys 1995, 102, 4931.
76. Facelli, J. C. J Phys Chem B 1998, 102, 2111.
77. Pearson, J. G.; Le, H.; Sanders, L. K.; Godbout, N.; Havlin, R. H.; Oldfield, E. J Am Chem Soc 1997, 119, 11941.
78. For review: (a) Oldfield, E. J Biomol NMR 1995, 5, 217; for a recent application, see, e.g., (b) Heller, J.; Laws, D. D.; Tomaselli, M.; King, D. S.; Wemmer, D. E.; Pines, A.; Havlin, R. H.; Oldfield, E. J Am Chem Soc 1997, 119, 7827.
79. Stahl, M.; Schöpfer, U.; Frenking, G.; Hoffmann, R. W. J Org Chem 1997, 62, 3702.
80. See, e.g., (a) Häser, M.; Ahlrichs, R.; Baron, H. P.; Weis, P.; Horn, H. Theor Chim Acta 1992, 83, 455; (b) Hedberg, K.; Hedberg, L.; Bühl, M.; Bethune, D. S.; Brown, C. A.; Johnson, R. D. J Am Chem Soc 1997, 119, 5314; (c) Bühl, M.; Curioni, A.; Andreoni, W. Chem Phys Lett 1997, 274, 231.
81. (a) Bühl, M. Unpublished results; for a description of methods and basis sets see, e.g., (b) Bühl, M. Chem Eur J 1998, 4, 734.
82. For review: Saunders, M.; Cross, R. J.; Jimenez-Vazquez, H. A.; Shimishi, R.; Khong, A. Science 1996, 271, 1693.
83. (a) Billups, W. E.; Gonzalez, A.; Gesenberg, C.; Luo, W.; Marriott, T.; Alemany, L. B.; Saunders, M.; Jimenez-Vazquez, H. A.; Khong, A. Tetrahedron Lett 1997, 38, 175; (b) Bühl, M.; Thiel, W.; Schneider, U. J Am Chem Soc 1995, 117, 4623; (c) Boltalina, O. V.; Street, J. M.; Taylor, R. J Chem Soc Perkin Trans 1998, 2, 649.
84. NICS stands for ''nucleus-independent chemical shift'': Schleyer, P. v. R.; Maerker, C.; Dransfeld, A.; Jiao, H.; Hommes, N. J. R. v. E. J Am Chem Soc 1996, 118, 6317.
85. Zhang, Y.; Pan, W.; Yang, W. J Chem Phys 1997, 107, 7921; Wesolowski, T. A.; Parisel, P.; Ellinger, Y.; Weber, J. J Phys Chem A 1997, 101, 7818.
86. Dunning, T. H. J Chem Phys 1989, 90, 1007.
87. Frisch, M. J.; Trucks, G. W.; Schlegel, H. B.; Gill, P. M. W.; Johnson, B. G.; Robb, M. A.; Cheeseman, J. R.; Keith, T.; Petersson, G. A.; Montgomery, J. A.; Raghavachari, K.; Al-Laham, M. A.; Zakrzewski, V. G.; Ortiz, J. V.; Foresman, J. B.; Peng, C. Y.; Ayala, P. Y.; Chen, W.; Wong, M. W.; Andres, J. L.; Replogle, E. S.; Gomperts, R.; Martin, R. L.; Fox, D. J.; Binkley, J. S.; Defrees, D. J.; Baker, J.; Stewart, J. P.; Head-Gordon, M.; Gonzalez, C.; Pople, J. A. Gaussian-94, Revision B.2, Gaussian: Pittsburgh, PA, 1995.
88. ACES-II program by J. F. Stanton, J. Gauss, J. D. Watts, W. J. Lauderdale, and R. J. Barlett, University of Florida, Gainesville, FL, 1994. We thank Prof. J. Gauss for providing a modified version.
89. Blügel, S.; Akai, H.; Zeller, R.; Dederichs, P. H. Phys Rev B 1987, 35, 3271.